River Flow 2010 - Dittrich, Koll, Aberle & Geisenhainer (eds) - © 2010 Bundesanstalt für Wasserbau ISBN 978-3-939230-00-7

Modeling composite river bank erosion in an alluvial river bend

Tapas Karmaker & Subashisa Dutta
Department of Civil Engineering, Indian Institute of Technology Guwahati, India

ABSTRACT: Composite river bank formation is quite common in large alluvial rivers and very high bank erosion rate is commonly reported in this type of formation. As of bank composition, cohesive layers of clay or silt formation are sandwiched by sand layers. Bank erosion processes involved are basal erosion at the toe of the bank, cantilever failure of the overhanging soil layers and deposition of the bank failure material. Factor safety of the cantilever failure also depends upon degree of saturation of the bank soil. Integrating all these bank erosion processes with hydrodynamic and morphological processes in a river bend, an analytical river model is proposed here. To demonstrate the model performance, a river bend with active bank erosion rate in the middle reach of Brahmaputra river in India has been considered. The soil erosion parameters such as critical shear stress and erodibility coefficients of cohesive layers were measured by submerged-jet test apparatus and seasonal bank erosion rate at a few locations of the bend were measured by repeated field survey using Differential Global Positioning System. The predicted seasonal bank erosion rate by the analytical model is compared with the field measured one. The results show the present analytical model works well for predicting the seasonal extent of bank erosion for the composite bank in a river bend. The model can be used to obtain morphological dynamics of a sand-bed river bend, accounting for variation in the bank material composition.

Keywords: Composite riverbank, Bank erosion, Cantilever failure, Critical shear stress

1 INTRODUCTION

High rate of bank erosion in the alluvial rivers has been of great concern, causing serious problems to the habitats, river and environmental engineers and others through loss of fertile land, danger to floodplain structures, increased downstream sedimentation, loss of valuables and lives (Muramoto et al., 1992; Mosselman et al., 1995; and Tingsanchali et al., 1997). Better understanding of the bank erosion mechanisms is essential for designing a cost-effective bank protection system(s). Being associated with so many controlling variables with uncertainty in the measurement, hydrodynamic and morphodynamic processes involved in the bank erosion are always difficult to be completely understood/modeled in a large river (Karmaker & Dutta, 2009a).

River bank erosion occurs mainly due to three processes: fluvial entrainment, sub-aerial erosion and mass failure due to poor strength of the bank materials (Lawler, 1995). One or the combination of these processes is responsible for the river bank erosion. The bank erosion for a homogeneous river bank is mainly dominated by a single process. Moreover, the nature of the erosion for a cohesive river bank is completely different from cohesionless (sand-bed) river bank. In a cohesive river bank, the erosion takes place as crumbs of soil rather than individual particles, as they are bound tightly by the electromechanical cohesive forces (Lawler et al., 1997). On the other hand the erosion in cohesionless river bank is due to loss of individual particles. The river bank erosion in case of composite river bank is even more complex. Banks of the alluvial river reaches are mostly composed of stratified soil layers, grain sizes of which vary from fine to coarse one. Normally, the alluvial river bed and the lower layers of composite banks are composed of cohesionless materials and the top layer of the bank is composed of stiff clay soil with vegetation cover.

Several studies have been carried out by the researchers to quantify and model the bank erosion

in a river. Field investigation of the composite bank erosion was carried out in the last two decades only. Hagerty (1991) carried out a study to show that the river bank erosion is not consistent with peak flood discharge; rather it may occur long after the peak flow especially for a composite riverbank. Due to the presence of the pervious clay layers, water seeps to the river from the bank and causes erosion. Theoretical study of the mechanical processes of channels with erodible banks was investigated initially by Ikeda et al. (1981) and Parker et al. (1982). Later the model of Ikeda et al. (1981) was improved by Blondeaux & Seminara (1985), who explained theoretically the resonance phenomenon between a bar and bend in a channel with erodible banks. All these theories assumed simple bank erosion model which considers the rate of bank line shifting is proportional to the excess near-bank flow velocity over the mean value. This concept cannot be applied to the channel with complex planform. Kovacs & Parker (1994), Nagata et al. (1996), and Duan et al. (1997) developed numerical schemes to simulate temporal changes in channel planforms due to bank erosion. All these models have been evaluated with the limited cases of laboratory flume studies with narrow, straight channel with non-cohesive banks. Darby & Thorne (1996) and Darby et al. (1996) developed the bank erosion model in which the rotational slip and planar bank failures were considered. Those two studies verified the model prediction with natural bank erosion rate.

Recent research on bank erosion model emphasizes on the fluvial erosion and finite element based seepage analysis due to the variation of pore water pressure (Rinaldi et al., 2004; Darby et al., 2007; Rinaldi et al., 2008). Those predictions were well validated with data from the natural river with composite bank. All the cases, the planar failure and/or cantilever failure were considered for bank stability analysis.

Duan (2005) developed an analytical approach to calculate the rate of bank erosion for cohesive soil. He related the bank erosion with the frequency of flooding and thus treated the erosion phenomenon as probabilistic approach. Chen & Duan (2006) solved the two dimensional depth averaged flow equations for a sine generated channel with bank erosion processes. They considered the rate of bank erosion as a net result of near bank sediment deposition and transport.

In spite of several advancements in the bank erosion modeling and monitoring, limited studies so far have been carried out for composite riverbank; especially for the alluvial riverbank which is mostly composed of sand, silt and clay in layers. There is no mathematical river model available till date for estimate the composite bank erosion rate. In the present study an analytical river model has been developed for the composite river bank considering the entrainment and deposition of the sediment particle from the bank surface, basal erosion due to excess shear stress, cantilever mass failure and near bank net sediment transport rate. The main objective was to couple the analytical bank erosion and bed degradation model (Chen & Duan, 2006) with erosion of the deposited sediment near bank in a river bend (Duan, 2005).

2 ANALYTICAL MODEL

2.1 *Fluvial erosion model*

The fluvial erosion rate can be quantified using the excess shear stress theory proposed by Partheiades (1965) and Arulanandan et al. (1980):

$$\varepsilon = k_d \left(\tau_b - \tau_c \right)^a \tag{1}$$

where ε = fluvial erosion rate per unit time, k_d = erodibility coefficient of the bank soil, τ_b = boundary shear stress for the cohesive soil, τ_c = critical shear stress and a = empirical exponent generally considered as 1.0. Total fluvial erosion (E) for time Δt can be computed as:

$$E = \omega' = \varepsilon \times \Delta t \tag{2}$$

Erodibility parameters are highly variable and difficult to estimate (Rinaldi et al., 2008). *In situ* submerged jet testing devices was used to estimate the erodibility parameters for the cohesive soils (Hanson & Simon, 2001). The bed shear stress can be estimated by using, $\tau = \gamma RS$, where, γ the unit weight of water, R the hydraulic radius, S the energy slope. Bank shear stress was estimated by using, $\tau_b = 0.76\gamma RS$, as suggested by Leutheusser (1963).

2.2 *Entrainment of the bank material deposited at toe*

The net average rate of bank erosion due to entrainment and deposition of the sediment particle can be given through the following analytical relation (Duan, 2005):

$$\overline{\xi} = E_1 \left(1 - \frac{\tau_{bc}}{\tau_{b0}} \right)^{3/2} \sqrt{\tau_{b0}} \tag{3}$$

where $\overline{\xi}$ = depth averaged erosion rate of the deposited material at toe, τ_{bc} = critical shear stress of the deposited material, τ_{b0} = shear stress at the toe

of the bank slope, E_1 coefficient can be defined as:

$$E_1 = \sin\overline{\beta}\sqrt{\frac{C_L^{'}}{3\rho_s}}\left(1-\frac{C}{C_*}\cos\overline{\beta}\right) \quad (4)$$

where $\overline{\beta}$ = average bank slope, $C_L^{'}$ = coefficient of lift force using friction velocity, C = depth averaged suspended sediment concentration, C_* = equilibrium suspended sediment concentration, ρ_s = density of sediment particle.

2.3 *Stability and cantilever failure*

Cantilever stability of the bank can be assessed by the combined effect of self weight, shear strength, tensile strength and the compressive strength of the bank materials. Three modes of failures can occur: (1) shear failure, (2) beam failure and (3) tensile failure. The factors of safety against these failures can be computed from the equations by Thorne & Tovey (1981):

$$F_{ss} = A\times\frac{(\beta-\chi)}{\beta}\times\frac{\beta}{2r} \quad (5)$$

$$F_{sb} = A\times\frac{\beta^2}{(1+r)B'} \quad (6)$$

$$F_{st} = A\times\frac{B}{(1-\beta)} \quad (7)$$

where F_{ss} = factor of safety against shear failure, F_{sb} = factor of safety against beam failure, F_{st} = factor of safety against tensile failure, r = ratio of the tensile strength to the compressive strength of soil. Other parameters can be written as:

$$A = \frac{\sigma_t}{\gamma b_1} \quad (8)$$

$$B = \frac{b_1}{H} \quad (9)$$

$$B^{'} = B\left(\frac{\beta}{\beta-\chi}\right)^2 \quad (10)$$

$$\beta = \left(\frac{H-l}{H}\right) \quad (11)$$

$$\chi = \left(\frac{m}{H}\right) \quad (12)$$

where H = overhang height of the bank, m = length of the upper crack, l = length of the lower desiccation crack, b_1 = width of the overhang bank.

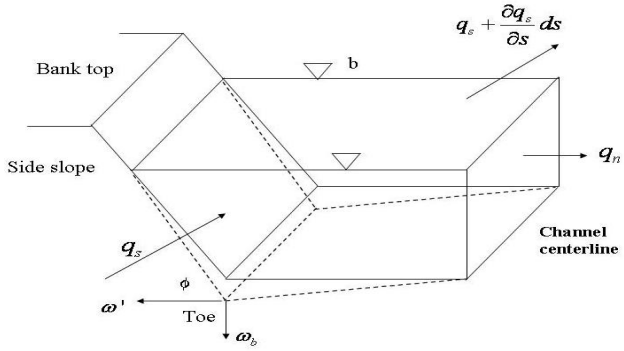

Figure 1. Sediment mass balance in the near bank control volume.

2.4 *Bed degradation model*

Bank advancement is caused by the deposition of the sediment at the bank. The bank retreat as it is eroded and transported away by the flow. Predicting bank advance or retreat is based on the mass conservation of the sediment in a control volume near the bank, including sediment from bank erosion and bank failure, sediment stored near the bed and sediment flux transported in and out from the control volume (Chen & Duan, 2006). The sediment continuity equation can be written as follows:

$$\left(q_s+\frac{\partial q_s}{\partial s}ds\right)b - q_s b + q_n ds = -\omega'\frac{h.ds}{2}(1-P)\rho_s$$

$$-\omega_b\frac{b.ds}{2}(1-P)\rho_s - \overline{\xi}\frac{dh}{\cos\theta}ds(1-P')\rho_{sand} \quad (13)$$

where ω' = lateral bank erosion rate at the toe per unit time in transverse direction, ω_b = bed degradation rate at the bank toe, ρ_{sand} = density of the sand from river bank, q_s and q_n = sediment transport rate component in longitudinal and transverse directions, P = porosity of cohesive soil, P' = porosity of the sandy deposits from the bank, θ = angle of repose of deposited soil mass at the bank toe, b = half width of the channel. Rearranging the above equation, we can write:

$$\omega_b = -\overline{\xi}\frac{2}{b}\frac{dh}{\cos\theta} - \omega'\frac{h}{b}\frac{(1-P)}{(1-P')}\frac{\rho_s}{\rho_{sand}}$$

$$-\frac{2}{b(1-P')\rho_{sand}}\left(\frac{\partial q_s}{\partial s}b+q_n\right) \quad (14)$$

2.5 *Empirical sediment transport*

In Eq. (14), the stream wise sediment transport rate can be computed using Leiwei bed-load equation (Chien et al., 1989). The equation is valid for a wide range of sediment particle grain size (D_{50} = 0.25-23mm) and the flow conditions (H/D = 5-500). After simplifying the final form of the equation can be given (Chen & Duan, 2006):

$$q_s = k_q U^4 \tag{15}$$

where U = reach average velocity and k_q can be given by:

$$k_q = \frac{2D_{50}^{1.25}}{g^{1.5}H^{1.75}} \tag{16}$$

where g = gravitational acceleration, H = reach average flow depth.

The first order derivative of q_s in the longitudinal direction can be expressed as:

$$\frac{\partial q_s}{\partial s} = k_q 4U^3 \frac{\partial U}{\partial s} \tag{17}$$

The conceptual diagram for the mass balance in the control volume is depicted in Figure 1. The transverse bed load transport rate can be given as the ratio as derived by Ikeda (1989) by analyzing the force balance of the moving spherical particle on a plane inclined to both the longitudinal and transverse direction:

$$C_s = \frac{q_n}{q_s} = \tan\varphi + \frac{1+\frac{C_L}{C_D}\mu}{\lambda\mu}\sqrt{\frac{\tau_c}{\tau}}\tan\psi \tag{18}$$

where φ = angle where the bed shear stress deviates from the longitudinal direction, $\tan\psi$ = transverse bed slope, μ = coefficient of the kinetic friction between the particle and can be considered as 0.43 (Kikkawa et al., 1976; Ikeda, 1989), λ = ratio of the kinetic friction coefficient to the static friction coefficient equals to 0.59 (Ikeda, 1989), τ_c and τ = critical and actual bed shear stresses respectively, C_D and C_L = drag and lift coefficients, can be considered as C_L/C_D = 0.85 for spherical particle (Kikkawa et al., 1976). Engelund (1974) expressed the direction of bed shear stress with the deviation angle can be given as:

$$\tan\varphi = \frac{\tau_n}{\tau_s} = 7.0\frac{h}{r_1} \tag{19}$$

where τ_n and τ_s are the bed shear stress in the transverse and longitudinal direction, h the flow depth, r_1 the local radius of curvature. After substituting the final form of the equation (18) can be rewritten as:

$$q_n = \left(7.0\frac{h}{r_1} + 5.382\sqrt{\frac{\tau_c}{\tau}}\tan\psi\right)q_s \tag{20}$$

A brief procedure of the steps involved in the present model is shown in a flow chart (Figure 2). Brief descriptions of critical parameters used in this model are presented in Table 1.

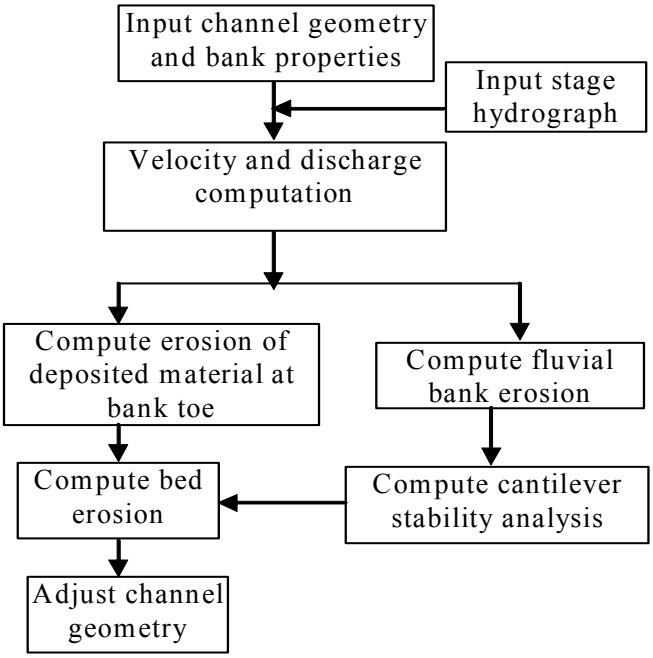

Figure 2. Process-based flow chart for bank erosion.

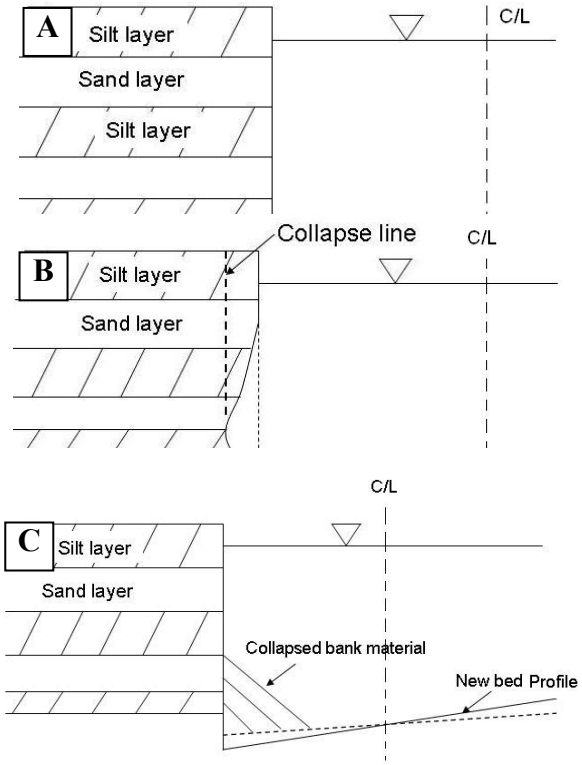

Figure 3. Schematic diagram of various stages of the bank erosion in a composite river bank. (a) Initial bank profile (b) progression of basal erosion (c) failure of the cantilever mass and its deposition near river bed with angle of repose along with bed degradation.

Table 1. Details of critical parameters used in the mathematical model with brief description.

Variable	Computational procedure	Value used
Erodibility coefficient, (k_d)	Through field experiments, e.g., submerged jet test	Site specific
Critical shear stress (τ_c)	Through field experiments	Site specific
Boundary shear stress (τ_b)	Computed from average energy slope and depth of flow	variable
Coefficient of lift force ($C_L^{'}$)	Reported value	0.178 for uniform sediment
Depth averaged actual suspended sediment concentration (C)	Measured *in situ*	450 mg/l
Equilibrium suspended sediment concentration (C_*)	Estimated from empirical equation, e.g., Yang's approach	600 mg/l
Ratio of the tensile strength to the compressive strength of soil (r)	Computed through laboratory experiments	Reported value 0.10
Tensile strength (σ_t)	Determined through the laboratory experiments of undisturbed samples	5000 Pa
Sediment transport rate component in longitudinal direction (q_s)	Determined from empirical equation, which depends on reach average velocity (U)	Valid for D_{50} = 0.25-23 and *Flow depth*/D_{50} = 5-500
Sediment transport rate component in transverse direction (q_n)	Fractional part of q_s estimated through empirical equation	--
Erosion rate of deposited sediment near toe, (ξ)	Computed based on near bank sediment transport rate, critical and developed shear stress angle of repose and coefficient of lift	--
Coefficient of the kinetic friction between the particles (μ)	Based on particle shape	0.43
Ratio of the kinetic friction coefficient to the static friction coefficient (λ)	Reported value	0.59

3 STUDY AREA

The study site is located along the Brahmaputra river (at Jamuguri, North Lakhimpur), North-East India. The site ($26^0 50'08"N, 93^0 46'08"E$) is about 70 km upstream of Tezpur town. Figure 4 shows the geographic location of the site. The river flows from east to west at this location. Morphological studies using multi-date satellite imagery (LISS-III) show that after 2004 extreme flood, a large river bend has been formed at the location. Till date the river bank is under severe threat of erosion. It also has been found from the satellite imagery study that a bank area of 2.4 km^2 was eroded out during the flood season of 2004. The radius of the centerline of the bend is about 2460 m and the channel widths at the upstream and downstream are 630 m and 1126m, respectively (Karmaker & Dutta, 2009a).

Detailed hydrographic and river bank survey was conducted twice: during the moderate flow condition and during high flood condition (water level nearly 1m higher than the bank full discharge) for the years 2007 and 2008. The survey includes the data collection like bathymetry using GPS aided Echo-sounder, velocity profile through ADCP, river bed and bank soil samples, depth averaged water samples for suspended sediment concentration. The measuring devices were mounted on an engine propelled vessel. The accuracy of the GPS instrument was +/-1.5 meters.

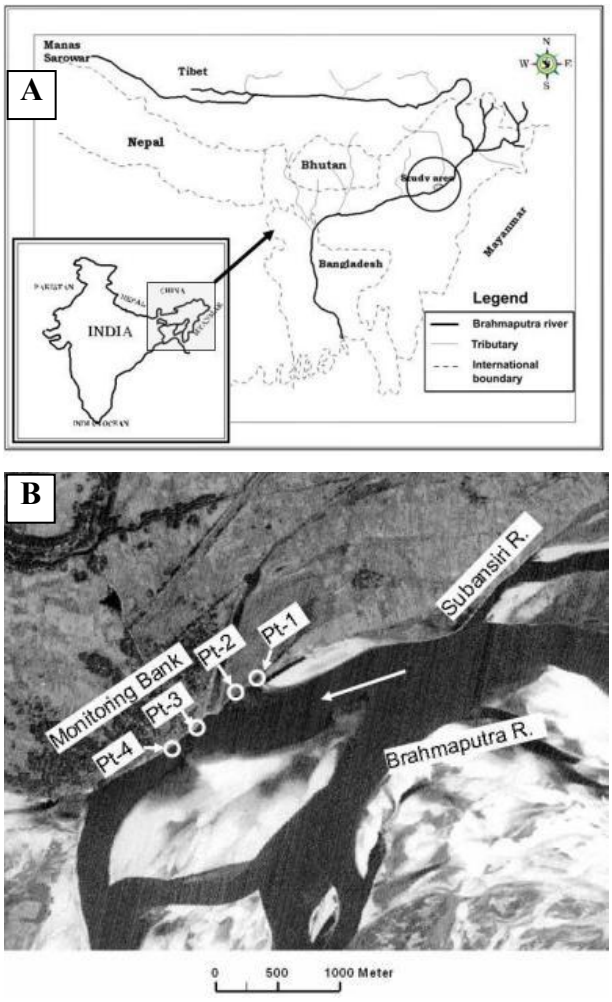

Figure 4. Study reach. (a) Index map. (b) Satellite imagery of the site in 2007 (Pt-1, Pt-2, Pt-3 and Pt-4 are the monitoring points for measuring bank erosion rate).

The eroding bank has an average height of 5 to 6 m. Although the thickness of different layers are variable, but the average composition can be described as (from top to the bottom): (1) a stiff cohesive layer with grass (thickness of 100-150 cm), (2) a layer of densely packed silt (thickness of 25-30 cm), (3) a layer of silty clay (thickness of 40-50 cm), (4) a layer of fine sand (40-50 cm), (5) a layer of sandy silt (thickness of about 300 cm), (6) below that a layer of silty clay at the bank toe.

4 RESULTS AND DISCUSSION

In the present study, the hydrographic data of year 2008 is used. The stage hydrograph in this type of a large river basin consist of multiple flood waves (Karmaker & Dutta, 2009b). Similar nature of flood hydrograph with flood waves can be found in Figure 5. The reach averaged observed velocity was considered to calibrate the model through the Manning's roughness factor.

4.1 *Cantilever stability*

The analysis of the cantilever failure for the monitoring point-4 will be discussed. The estimated factors of safety for three types of cantilever failure, as given in Figure 5, indicate that among the four cases of mass failure, beam type of failure occurred three times and one case is for shear failure. Although it was reported by Thorney & Tovey (1981), that the shear failure is the most common type of cantilever bank failure. No case of tensile bank failure was found from this simulation. Moreover, the simulated factors of safety fall within the comparable limit for beam and shear type of failure cases.

4.2 *Bank erosion*

The cumulative bank erosions at the four different monitoring points are compared with the observed bank erosion rate. Figure 6 shows the simulated seasonal cumulative bank erosion. The sudden increase in the erosion indicates the cantilever mass failure. Results indicate the variability of the time of failure of the bank in spite of the monitoring points not so far apart. Fluvial erosion is the key factor prior to the cantilever failure in this model. So the higher critical shear stress, lower the fluvial erosion and longer cantilever stability. Among the four monitoring points, the critical shear stress at Point-2 is quite high and about 10 N/m^2. During the entire period no seasonal bank erosion was found at that point. It was also observed that the cantilever failure lagged well behind the flood peaks. Similar nature of bank failure was confirmed from the local people during the field survey. However, the lag time could not be compared due to the absence of the temporal *in-situ* bank erosion data.

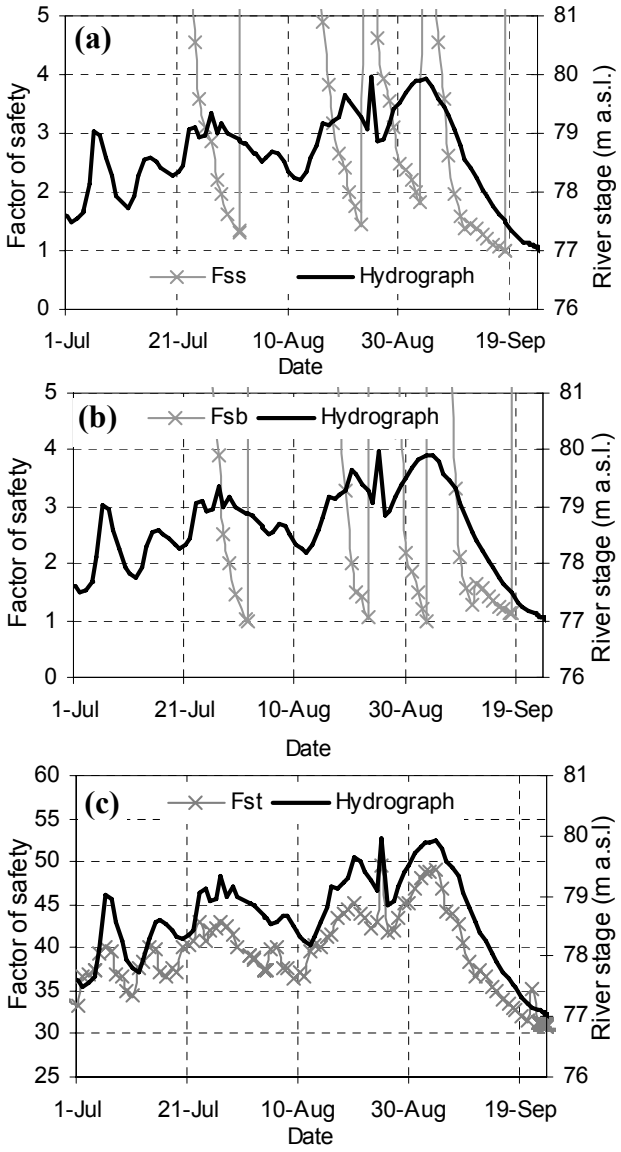

Figure 5. Temporal variation of factors of safety in cantilever bank failure. (a) For shear failure, (b) for beam failure and (c) tensile failure

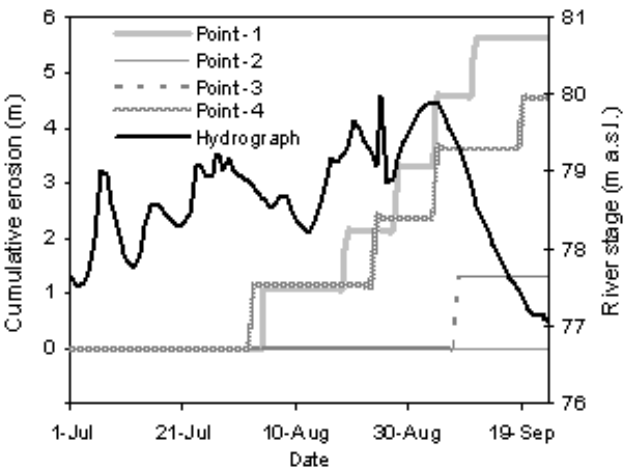

Figure 6. Predicted cumulative bank erosion for four monitoring points

Total seasonal bank erosion at the four monitoring points are shown in Table 2. The model predicts little higher for the observation points 1 and 4, but slightly under predicts for point 3. Apart from the various types of erosion considered in the present model, there may be seepage erosion, which is quite common for composite bank (Wilson et al., 2007; Fox et al., 2007). The under predicted result may be justified as the presence of seepage erosion, which was observed during the field survey. There was no erosion at the monitoring Point-2. Interestingly, similar result is predicted by the model.

Table 2. Comparison of the observed and computed bank erosion in four monitoring points.

Location	Observed erosion (m)	Computed erosion (m)
Pt-1	4.8	5.63
Pt-2	0	0
Pt-3	2.85	1.28
Pt-4	3.72	4.54

5 CONCLUSION

This paper presents a bank erosion model in a river bend addressing the basal erosion due to hydraulic force, all possible types of cantilever failure of the overhang soil mass, the erosion of the deposited bank material at the toe of the bank after cantilever failure and the bed degradation. It also computes the near bank sediment concentration by considering sediment transport and mass failures. The study shows that the fluvial erosion of the cohesive layers found to be the critical processes in the selected river reach. Nevertheless, seepage erosion is also an important part of the bank erosion in the composite banks, which needs to be included in the present model in near future.

REFERENCES

Arulanandan, K., Gillogley, E., Tully, R. 1980. Development of a quantitative method to predict critical shear stress and rate of erosion of natural undisturbed cohesive soils. Rep. GL-8-5, U. S. Armay corps of Eng., Waterways Exp. Stn., Vicksburg,. Mississippi.

Blondeaux, P., Seminara, G. 1985. A unified bar-bend theoryof river meander. J. Fluid Mech., Cambridge, U. K., 157, 449-470.

Chen, D., Duan, J. G. 2006. Modeling width adjustment in meandering channels. J. Hydrol., 321, 59-76.

Chien, N., Zhang, R., Chou, Z. D. 1989. River evolution. Chinese Scientific Press, Beijing, China (in Chinese).

Darby, S. E., Thorne, C. R. 1996. Numerical simulation of widening and bed deformation of straight sand-bed rivers. I: Model development. J. Hydr. Eng., ASCE, 122(4), 184-193.

Darby, S. E., Thorne, C. R., Simon, A. 1996. Numerical simulation of widening and bed deformation of sand-bed rivers. II: Model evaluation. J. Hydr. Engrg., ASCE, 122(4), 194-202.

Darby, S. E., Rinaldi, M., Dapporto, S. 2007. Coupled simulation of fluvial erosion and mass wasting for cohesive river banks. J. Geophys. Res., 112, F03022; DOI: 10.2029/2006JF000722.

Duan, J. G. 2005. Analytical approach to calculate rate of bank erosion. J. Hydrau. Eng., 131(11), 980-990; DOI: 10.1061/(ASCE)0733-9429(2005)131:11(980)

Duan, G., Jia, Y., Wang, S. 1997. Meander process simulation with a two dimensional numerical model. Proc., Conf. on Mgmt. of Landscapes Distributed by Channel Incision, University of Mississippi, Miss., 389-394.

Engelund, F. 1974. Flow and bed topography in channel bends. J. Hydr. Div., ASCE, 100(HY11), 1631-1648.

Fox, G. A., Wilson, G. V., Simon, A., Langendoen, E., Akay, O, Fuchs, J. W. 2007. Measuring streambank erosion due to ground water seepage: correlation to bank pore water pressure, precipitation and stream stage. Earth Surf. Processes Landforms, 32, 1558-1573; DOI:10.1002/esp.1490.

Hagerty, D. J. 1991. Piping/sapping erosion. I: Basic considerations. J. Hydraul. Eng., 117(8), 991-text]

Hanson, G. J., Simon, A. 2001. Erodibility of cohesive streambeds in the loess area of the midwestern USA. Hydrol. Processes, 15, 23-38, doi:10.1002/hyp.149.

Ikeda, S., Parker, G, Sawai, K. 1981. Bend theory of river meanders. Part 1. Linear development. J. Fluid Mech., Cambridge, U.K., 112, 363-377.

Ikeda, S. 1989. Sediment transport and sorting at bends. In: Flow in Meandering Channels. (Eds.) Ikeda, S., Parker, G. American Geophysical Union, 103-125.

Karmaker, T., Dutta, S. 2009a. Predicting vulnerable bank erosion zones in a large river meander. Proc. Water, Environment, Energy and Society (WEES)-2009, New Delhi. pp 1670- 1676.

Karmaker, T., Dutta, S. 2009b. Generation of synthetic flood hydrograph in a large river basin. J. Hydrology. doi:10.1016/j.jhydrol.2009.12.001.

Kikkawa, H., Iheda, S., Kitagawa, A. 1976. Flow and bed topography in curved open channels. J. Hydraul. Divn., ASCE, 109(9), 1327-1342.

Kovacs, A., Parker, G. 1994. A new vectorial bedload formulation and its application to the time evolution of straight river channels. J. Fluid Mech., Cambridge, U. K., 267, 153-183.

Lawler, D. M., 1995. The impact of scale on the processes of channel-side sediment supply: A conceptual model. In: Effects of scale on Interpretation and Management of Sediment and Water Quality (Proc. of a Boulder Symp.). IAHS Publ. 226, Wallingford, U.K.: International Assoc. of Hydrological Science, 175-184.

Lawler, D. M., Thorne, C. R., Hooke, J. M. 1997. Bank erosion and stability. In Applied Fluvial Geomorphology for River Engineering and Management, (Eds.) Thorne, C.R. et al., 137-172. J. Wiely, Chichester, U. K.

Leutheusser, H. J. 1963. Turbulent flow in rectangular ducts. J. Hydraul. Div. ASCE., 89, 1-19.

Mosselmann, E., Huisink, M., Koomen, E., Seijmonsbergen, A.C. 1995. Morphological changes in a large braided sand-bed river. River Geomorphology, E. J. Hickin, ed., Wiely, Chiehester, U.K., 235-247.

Muramoto, Y., Fujita, Y. 1992. Recent channel processes of the major rivers in Bangladesh. Annuals of the Disaster Prevention Res. Inst., Kyoto, Japan, 35 B-2, 89-114 (in Japanese.

Nagata, N., Hosoda, T., Muramoto, Y. 2000. Numerical analysis of river channel processes with bank erosion. J. Hydr. Engrg., ASCE, 126(4), 243-252.

Parker, G., Sawai, K., Ikeda, S. 1982. Bend theory of river meanders. Part 2. Nonlinear deformation of finite-amplitude bends. J. Fluid Mech., Cambridge, U.K., 115, 303-314.

Partheiades, E. 1965. Erosion and deposition of cohesive soils. J. Hydraul. Div. ASCE, 91, 105-139.

Rinaldi, M., Casagli, S., Dapporto, Gargini, A. 2004. Monitoring and modelling of the pore water pressure changes and riverbank stability during flow events. Earth Surface Processes Landforms, 29, 237-254; DOI: 10.1002/esp. 1042.

Rinaldi, M., Mengoni, B., Luppi, L., Darby, S. E. 2008. Numerical simulation of hydrodynamics and bank erosion in a river bend. Water Resour. Res., 44, W09428; DOI:10.1029/2008WR007008.

Thorney, C. R., Tovey, N. K. 1981. Stability of composite river banks. Earth Surf. Processes landforms, 6, 469-484; DOI:10.1002/esp.3290060507

Tingsanchali, T., Chinnarasri, C. 1997. Design of Mekong river bank protection. Proc. Conf. on Mgmt. of Landscapes Distributed by Channel Incision, University of Mississippi, Miss., 345-348.

Wilson, G. V., Periketi, R.K., Fox, G. A., Dabney, S. M., Shields, F. D., Cullum, R.F. 2007. Soil properties controlling seepage erosion contributions to streambank failure. Earth Surf. Processes Landforms, 32, 447-459; DOI: 10.1002/esp.1405.